of these proteolytic enzymes are identical to those found with the carboxypeptidase altered aldolase. All of the degraded enzymes are equally depressed in the ability to catalyze the detritiation of labeled DHAP (*5*), consistent with the conclusion that a single step in the overall process has been affected.

Although several proteolytic enzymes with different specificities produce the same changes in the catalytic properties of aldolase, this enzyme should not be considered as a structure so delicately poised that every peptide bond is essential to maintain the most efficient catalyst. Aldolase-T, prepared by Szabolcsi and associates (*16*) by treatment of a *p*CMB derivative of aldolase with trypsin, has only slightly reduced activity in the usual assay and shows only a proportional loss in the detritiation reaction (*17*).

ALAN H. MEHLER
MARSHALL E. CUSIC, JR.
Department of Biochemistry, Marquette University School of Medicine, Milwaukee, Wisconsin 53233

References and Notes

1. O. Meyerhof, K. Lohmann, P. Schuster, *Biochem. Z.* **286**, 301, 319 (1936).
2. I. A. Rose and S. V. Reider, *J. Am. Chem. Soc.* **77**, 5764 (1955); B. Bloom and Y. J. Topper, *Science* **124**, 982 (1956).
3. E. R. Drechsler, P. D. Boyer, A. G. Kowalsky, *J. Biol. Chem.* **234**, 2627 (1959).
4. W. J. Rutter, O. C. Richards, B. M. Woodfin, *ibid.* **236**, 3193 (1961).
5. I. A. Rose, E. L. O'Connell, A. H. Mehler, *ibid.* **240**, 1758 (1965).
6. G. R. Bartlett, *ibid.* **234**, 449 (1959).
7. W. Mejbaum, *Z. Physiol. Chem.* **258**, 117 (1939).
8. Z. Dische, *Ann. N.Y. Acad. Sci.* **75**, 129 (1958).
9. A. H. Mehler, *J. Biol. Chem.* **238**, 100 (1963).
10. A. Ginsburg and A. H. Mehler, *Biochemistry* **5**, 2623 (1966).
11. D. E. Koshland, Jr., *Science* **142**, 1533 (1963).
12. W. P. Jencks, *Ann. Rev. Biochem.* **32**, 639 (1963).
13. F. C. Hartman and R. Barker, *Biochemistry* **4**, 1068 (1965).
14. I. A. Rose *Ann. Rev. Biochem.* **35**, 23 (1966).
15. Kindly given to us by Dr. Martin Ottesen of the Carlsberg Laboratories.
16. E. Biszku, L. Boross, G. Szabolcsi, *Acta Physiol. Acad. Sci. Hung.* **25**, 161 (1964).
17. Unpublished experiments of Dr. G. Szabolcsi, Institute of Biochemistry, Hungarian Academy of Science, while she was a visiting scientist in the laboratory of one of us (A.H.M.) at the National Institutes of Health in 1964.
18. Supported by NSF grant No. GB-4084. The technical assistance of Mrs. Carol Cramer is gratefully acknowledged.

5 January 1967

Fossil Alpha-Particle Recoil Tracks: A New Method of Age Determination

Abstract. *The discovery of a new type of fossil nuclear track in mica is reported. This track is produced by the recoil nucleus accompanying the α-particle decay of uranium and thorium impurities. The tracks are very short and can be seen with phase contrast microscopy. Measurement of fossil α-recoil track densities, coupled with determinations of the thorium and uranium contents, provides a new dating technique analogous to the previously discovered "fission-track method." The primary advantage of the α-recoil method is a several-thousand-fold increase in sensitivity over the fission-track technique. The α-recoil method should also prove useful in studying the problem of extinct isotopes in meteorites.*

It has been known for some time that fission fragments from the spontaneous fission of U^{238} produce stable-track latent images in a variety of materials (*1, 2*). These latent images can be developed by a chemical etching technique to the point where they are easily visible in an ordinary optical microscope. Measurement of the density of ancient (fossil) tracks followed by a reactor irradiation and a subsequent track count forms the basis of the "fission-track dating method" that has been successfully applied to a variety of terrestrial samples ranging in age from 20 years to 1.5×10^9 years. In meteorites, excess fission tracks (defined as the number of tracks over and above the number expected from spontaneous fission of U^{238}), have been interpreted as arising (*3*) from the spontaneous fission of the now-extinct isotope Pu^{244}. Using phase contrast microscopy we have seen a new kind of fossil track. Figure 1A shows a normal fission track in etched mica observed with transmitted light. Figure 1B shows the same sample illuminated with a Zernicke phase-contrast system in a Leitz microscope. Numerous shallow etch pits, invisible in normal illumination, are apparent in the phase-contrast picture. These shallow pits are in reality very short etched tracks.

That the small tracks are produced by the heavy recoil nuclei accompanying α-particle emission of uranium and thorium impurities is shown by the following: (i) The ratio of small tracks to spontaneous fission tracks is approximately constant in samples with very different uranium concentrations; (ii) the depth of the shallow pits, or track lengths, inferred on the basis of the α-recoil hypothesis agrees with the experimental value obtained by electron microscopy; (iii) the measured length is also compatible with the theoretical range of α-recoils; and (iv) an α-emitter, Th^{228}, placed next to annealed mica produces new shallow pits with the proper frequency.

Fossil fission tracks are produced almost completely by U^{238}. On the other hand, α-recoil tracks are produced by both U and Th. The ratio of small tracks to fission tracks should thus be expected to vary for different samples depending on Th/U ratio. However, since the ratio of Th to U does not vary much in nature (*4*), one might expect to find a roughly constant ratio of α-recoil to fission tracks. To check this point we made track counts in five samples of muscovite mica etched for 2 hours at 20°C in 48 percent hydrofluoric acid, and in one sample of phlogopite mica etched for 60 seconds in the same solution. Although the fission-track density varied by a factor of 30, ranging from 5×10^2 cm^{-2} to 1.5×10^4 cm^{-2}, the ratio of small tracks to large tracks was approximately constant, varying from 2.3×10^3 to 4.5×10^3 with an average value of 3.5×10^3.

Only tracks that intersect a free surface can be revealed by the acid attack. The density of revealed tracks is thus proportional to the etchable track length. Specifically the density of fission tracks is given with reasonable precision by the following relation (*2*)

$$\rho_f = N_o C_U \lambda_f(U) T R_f \qquad (1)$$

where λ_f (U) is the decay constant for spontaneous fission, C_U is the concentration of uranium, R_f is the total etchable range of the two fragments emitted in a single fission, T is the time and N_0 is the number of atoms per cubic centimeter.

The corresponding relation for the density of α-recoil tracks is

$$\rho_\alpha = N_o C_U \lambda_\alpha(U) T R_\alpha + N_o C_{Th} \lambda_\alpha(Th) T R_\alpha \qquad (2)$$

If the α-recoil ranges for Th and U are identical and if the ratio of Th to U is 4 (4), the measured value of $(\rho_\alpha/\rho_f) = 3.5 \times 10^3$ gives $R_\alpha = 125$ Å.

This calculated value for the etchable track length must agree with the directly measured track length if the α-recoil hypothesis is correct. To investigate this point, we made shadow replicas of an etched mica surface. The sample was shadow-cast with Pt at 30°, then coated with polyacrylic acid and stripped. The sample was then backed with carbon, and the acid film was dissolved away.

Measurements on 26 pits gave depths ranging from 70 Å to 150 Å with an average value of ~ 100 Å. Considering the uncertainties involved, this is in excellent agreement with the above value of R_α calculated from the ratio of the track densities.

The theoretical range of a single α-recoil, calculated from the theory of Linhardt and Scharff (5), is 195 Å. The root-mean-square (r.m.s.) value of the total displacement resulting from the cascade of eight α-particles after the initial decay of U^{238} is about three times this value. The measured average range is thus less than the theoretical range by a factor of about 4. This implies, not surprisingly, that the etchable range, R_α, is less than the true range of the particles.

As a final check on the α-recoil hypothesis we attempted to produce the shallow pits directly in mica by bombarding annealed samples with α-recoil nuclei. Two experiments were performed. In the first, a sample of mica, annealed for 21 hours at 600°C, was placed in contact with a U foil and exposed in vacuum for 12 days. In the second experiment, solutions containing three different concentrations of Th^{228} were evaporated on annealed mica samples and then rinsed and etched after a 20-hour exposure. The annealing treatment had reduced the background α-recoil track density to ~ 200 cm^{-2}. As shown in Fig. 2, a striking positive effect was found in the Th^{228} experiment. Shallow pits, identical in appearance to those of the fossil pits, were produced in profusion in the mica in direct proportion to the concentration of Th^{228} on the samples.

Surprisingly, no new shallow pits were observed in the U-foil experiment, although the calculated density of recoils was orders of magnitude higher than the background. A trivial explanation for this negative result is simply that a surface film prevented the recoils from entering the mica. A more interesting possibility is that the damage produced by a single recoil is insufficient to nucleate the growth of an etch pit. In a natural sample an initial α-decay of U^{238} is followed by seven other α-decays in a chain. In a 12-day experiment, however, essentially only a single α-recoil is produced by either a U^{238} or U^{234} decay, the half-lives of the daughter products being very long. The situation with Th^{228} is different. The initial α-decay gives Ra^{224} which, in turn, disintegrates by α-decay with a half-life of 3.60 days. In a time short compared with this, there is an additional cascade of three α-particles. Thus, in the 20-hour experiment with TH^{228}, a significant number of events involved five recoils in succession—a situation closely analogous to that of fossil recoils in nature. Unfortunately, our monitoring of the absolute α-activity of the evaporated Th^{228} was not sufficiently accurate to determine whether the full five recoils are necessary to nucleate the acid attack or whether a single recoil will suffice.

We have also found that the apparent density of small pits varies with etching time, a saturation value being reached after about 2 hours of etching. The result may also indicate the presence of nucleation effects in which some damage sites, presumably with a high local concentration of defects, start to grow to a visible size at an earlier time than other, less heavily damaged sites.

One final point concerning the positive identification of the shallow etch pits with short α-recoil tracks needs to be considered. All the results outlined could equally well be explained by supposing that the α-particles themselves produce isolated small regions of radiation damage that nucleate the etch pits. This possibility can be eliminated by comparing the number of shallow pits per incident α-particle produced in the Th^{228} experiment, where α-particles and recoil nuclei were both present, with the value measured in an independent experiment with Po^{210}. In the Po^{210} experiment, the mica sample was separated from the source by an air gap sufficient to stop the recoils but not the α-particles. The samples placed next to the U foil were also certainly irradiated by copious numbers of α-particles. The U foil and Po^{210} experiments gave ratios of shallow pits

Table 1. Accumulated α-recoil densities for different ages.

Age (10^9 yr)	α-Recoil densities (relative units)*			
	U^{238}	U^{235}	Th^{232}	Total
1	0.166	0.012	0.192	0.37
2	.359	.043	.404	.81
3	.585	.126	.620	1.33
4	.859	.355	.876	2.09
4.6	1.03	.626	1.03	2.69

* Th/U ratio assumed equal to 4 in contemporary sample.

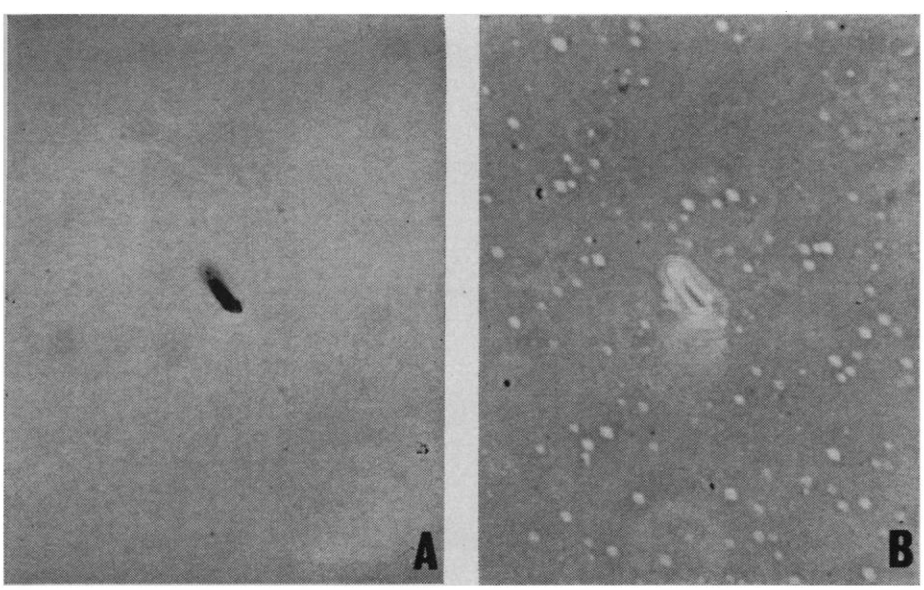

Fig. 1. Fossil tracks in muscovite mica etched for 2 hours at 20°C in 48 percent hydrofluoric acid. (A) A fission track in the center of the field of view taken in normal bright field illumination. (B) The same area as seen in phase contrast. In addition to the fission track, many shallow etch pits (α-recoil tracks) are now visible.

per incident α-particle of $< 5 \times 10^{-5}$ and $< 5 \times 10^{-7}$ respectively. The corresponding number for the Th^{228} was ~ 0.3. In view of the crude technique used for monitoring α-particles, the absolute values of these ratios are uncertain to at least a factor of ten. The qualitative conclusion is however clear; α-particles alone do not produce large densities of shallow etch pits.

The observation of α-recoil tracks has a number of interesting implications. The most obvious use of such tracks is in dating samples in a way analogous to the fission-track method. The advantage of the α-recoil method is the increase in track density, and hence sensitivity, by a factor of about 4×10^3. Although man-made objects have been dated by the fission track method, the overwhelming majority of relatively young samples contain too little uranium to give measurable ages. The high density of α-recoil tracks removes this limitation and permits, in principle, age measurements of any man-made sample containing a typical uranium concentration of one part per million. The dramatic increase in sensitivity also gives the promise of our being able to date the apatite crystals found in teeth—a problem that has not been solved by the fission-track approach, because of the low uranium concentrations in interesting samples. The large densities also should make it possible to date very small crystals such as those found in clay minerals.

Even in samples with measurable fission track ages, it may prove very useful to determine the α-recoil ages independently. A heating experiment in which a muscovite sample was held at 425°C in an argon atmosphere for 1 hour, indicates that α-recoil tracks are more resistant to thermal fading than fission tracks (90 percent retained versus 70 percent). Concordant fission and α-recoil ages would lend confidence to any determination of age; discordant ages, on the other hand, might be used to probe the geothermal history of various specimens.

Measurement of α-recoil ages in meteorites should also prove very useful in connection with the problem of extinct Pu^{244}. Certain meteorites have densities of fossil fission-tracks far in excess of the number that can be attributed to the spontaneous fission of U^{238}. These excess tracks were either produced by the spontaneous fission of Pu^{244} that was still present when the meteoritic minerals were formed or by the cosmic-ray–induced fission of heavy-element impurities. The problem of distinguishing between these two alternatives is discussed by Fleischer *et al.* (*6*) who show that the best method is to examine the excess track densities in different mineral phases, each possessing different track-fading properties. With this method, strong evidence for the prior existence of Pu^{244} has been found in the iron meteorite Toluca. The method is, however, not foolproof, since it is possible to "invent" a history (admittedly bizarre) for the meteorite such that a cosmic-ray effect simulates the behavior expected for Pu^{244}.

Because Pu^{244} has a relatively short half-life ($T_{1/2} = 8.2 \times 10^7$ years), meteorite crystals containing numerous tracks from the spontaneous fission of this isotope must have formed early in the history of the solar system. This point can be independently checked in meteorite crystals by measuring the α-recoil track age. This method is particularly sensitive for old samples because the number of α-recoils per uranium atom increases as one goes back in time owing to the increasing contribution of U^{235}. In Table 1 we give the total contributions of α-recoil from different isotopes for samples of different ages. The α-recoil contribution per unit time is about 3 times greater at the beginning of the life of a sample that is 4.6×10^9 years old than at the end. An old α-recoil age does not, itself, prove the prior existence of Pu^{244}; it is, however, a necessary condition for the Pu^{244} interpretation and the α-recoil age must be compatible with the fission-track densities attributed to the Pu^{244}.

Probably the tracks of α-recoils and fission fragments are produced by different radiation-damage processes. Fission fragments lose most of their energy in ionization and excitation, leading, in one view (*7*), to an "ion-explosion spike" that is responsible for the disruption of the solid. In contrast, recoil

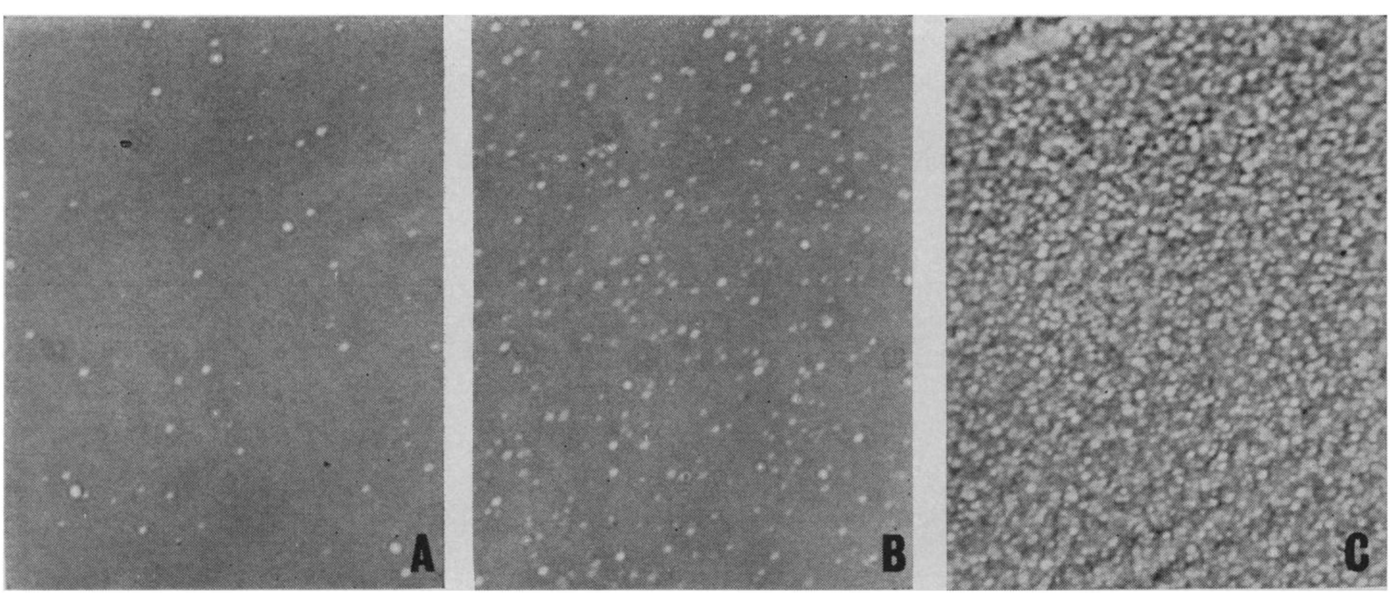

Fig. 2. Thorium-228 bombardment of annealed mica. Solutions containing different concentrations of Th^{228} were placed on annealed mica samples and dried. The samples were rinsed and etched in hydrofluoric acid after an irradiation for 20 hours. Phase-contrast microscopy shows numerous shallow etch pits, similar to the background etch pits in the unannealed sample. In the photographs the concentration of the Th^{228} increases from left to right, being respectively 1 (A), 10 (B), and 100 (C) in arbitrary intensity units.

nuclei accompanying α-decay have such low kinetic energies (500 ev/nucleon) that they are essentially unstripped; these particles lose their energy in elastic, hard-sphere collisions between atoms, rather than in electronic processes. The radiation damage produced by α-recoils is probably best described by the "displacement-spike" concept (*8*). Measurements of track formation by recoils of different energy, slowed down perhaps by a thin air gap, and of different mass—produced, for example, by accelerator-scattering experiments—should elucidate the details of the solid state processes involved.

Much work needs to be done in order to establish the utility of α-recoil tracks. The α-recoil track-dating method, for example, requires the determination of the Th/U ratio. Although this determination can be made in principle with the track methods, with the use of independent irradiations in fast and thermal neutron fluxes, the precise techniques remain to be developed. The α-recoil tracks are also very small and not as unique in appearance as the larger fiission tracks; thus it remains to be shown that the full increase in sensitivity for age measurement, that is possible in principle, can be realized in practice. It further remains to be shown that α-recoils can be found in other substances; particularly, for archeological investigations, in glass.

W. H. HUANG
Department of Earth Sciences,
R. M. WALKER
Laboratory for Space Physics,
Washington University,
St. Louis, Missouri

References and Notes

1. P. B. Price and R. M. Walker, *Nature* **196**, 732 (1962); R. L. Fleischer, P. B. Price, R. M. Walker, *Science* **149**, 383 (1965); *Annu. Rev. Nuc. Sci.* **15**, 1 (1965).
2. P. B. Price and R. M. Walker, *J. Geophys. Res.* **68**, 4847 (1963).
3. R. L. Fleischer, P. B. Price, R. M. Walker, *ibid.* **70**, 2703 (1965).
4. See for example, S. Heier and J. J. Rogers, *Geochim. Cosmochim. Acta* **27**, 137 (1963).
5. J. Linhard and M. Scharff, *Phys. Rev.* **124**, 128 (1961).
6. R. L. Fleischer, P. B. Price, R. M. Walker, M. Maurette, *J. Geophys. Res.*, in press.
7. R. L. Fleischer, P. B. Price, R. M. Walker, *J. Appl. Phys.* **36**, 3645 (1965).
8. See for example, J. Dienes and G. Vineyard, *Radiation Effects in Solids* (Interscience, New York, 1957).
9. We thank J. Kardos for the preparation and examination of the electron-microscopy specimen. The use of Th^{228} was suggested by A. Wahl, and the experiment was carried out in cooperation with D. Sarantides. The cooperation of W. Johns was also essential. Supported by McDonnell Aircraft contract P.O. Z60046T.

12 January 1967

Retinal Ganglion Cells: Specification of Central Connections in Larval Xenopus laevis

Abstract. *In a series of* Xenopus *larvae (stages 28 to 35), the left eye cup was dorsoventrally and anteroposteriorly inverted. After metamorphosis, the retinotectal projection was mapped by recording action potentials evoked in the tectum by a small spot of light projected on the retina. Normal retinotectal projection was found following rotation of the eye cup at stage 28 to 29. Rotation of the eye cup at stage 30 resulted in anteroposterior inversion of the retinotectal projection; rotation at stages 31, 32, and 35 resulted in inversion of the projection in anteroposterior and dorsoventral axis of the retina. Therefore the retinal ganglion cells were unspecified at stage 28 to 29; spatial specification of ganglion cells occurred in the anteroposterior axis of the eye cup at stage 30 and in the dorsoventral axis between stages 30 and 31.*

The time of retinal specification has been studied in amphibians in which the eye cup is rotated 180° at different stages of development before formation of the optic nerve, and by observation of the visuomotor behavior of these animals after maturation. Rotation of the eye cup of the salamander *Amblystoma* before larval stage 34 (*1*) or of the newt *Triturus* before larval stage 22 (*2*) does not alter the development of normal visuomotor behavior, but rotation after these developmental stages results in reversal of visuomotor reflexes. The inference from these experiments is that, during "functional polarization" (*1*) or "functional specification" (*2*) of the retina, the retinal ganglion cells acquire an unknown kind of local property enabling them to connect with the appropriate places in the tectum. As a result, the retinal ganglion cells connect with the optic tectum in the retinotopic order found in adult amphibians (*3*). I have determined the patterns of connections between retina and tectum which form after the eye cup of the clawed toad *Xenopus laevis* is rotated at different stages of development.

In 52 larvae of *Xenopus laevis* at different stages from 28 to 35 (*4*) the left eye cup was excised, rotated 180°, and reimplanted so that the dorsoventral and anteroposterior axes were inverted. The operation was performed before the development of any nervous connections between the eye and the brain.

Only 12 animals survived metamorphosis. The left eye had been rotated at stage 28 to 29 in six, in three at stage 30, and in one each at stages 31, 32, and 35. These animals were used for mapping the projection from the rotated left eye and from the normal right eye to the optic tectum.

The mapping procedure was as follows. The animal was anesthetized by immersion in an aqueous solution (1:1000) of tricaine methanesulphonate (MS 222-Sandoz) and paralyzed with an injection of 0.01 mg of tubocurarine chloride. The cranium was opened over the tectum, and the meninges covering the tectum were removed. The animal was fixed in position with its left eye centered on the axis of a projection perimeter at a distance of 33 cm from the perimeter arc. By means of the perimeter, a spot of light (subtense 1°, duration 1 second, spot luminance 60 cd/m^2, background luminance about 20 cd/m^2) could be moved to any position in the visual field of the eye being stimulated. Action potentials evoked by the light were recorded from the tectum by means of a platinum-iridium microelectrode (*5*) with a tip diameter of about 1 μ. A micromanipulator moved the electrode to a succession of positions 200 μ apart on the tectum. The electrode penetrated the tectum vertically to a depth of between 0 and 50 μ. The depth was uncertain because of dimpling of the tectum by the electrode. At each electrode position, the position of the stimulating light was adjusted until responses of maximum amplitude were evoked in the tectum. The responses had latencies varying from 30 to 60 msec and consisted of bursts of action potentials occasionally from one, but usually from several units. The responses could be evoked from within a region subtending from 5° to 15° in the visual field. After the projection from the left (rotated) eye was mapped to the right tectum, the animal was positioned with its right (normal) eye centered on the perimeter, and the